Environmental Science & Technology

Article

pubs.acs.org/est

The Chromium Detoxification Pathway in the Multimetal Accumulator *Silene vulgaris*

Ana Elena Pradas del Real,*[,†,§] Araceli Pérez-Sanz,[†] Mª.Carmen Lobo,[†] and David H. McNear, Jr.[‡]

[†]Dpto. de Investigación Agroambiental, IMIDRA, Finca "El Encín", A-II Km, 38.200, 28800, Alcalá de Henares, Madrid, Spain

[‡]Rhizosphere Science Laboratory, University of Kentucky, Department of Plant and Soil Sciences, 1100 Nicholasville Road, Lexington, Kentucky 40546, United States

Supporting Information

ABSTRACT: Phytomanagement could be a viable alternative in areas polluted with wastes from chromium-using industries. This study investigated the ability of *Silene vulgaris* to take up Cr(III) and Cr(VI) with special attention on the mechanism used by this species to tolerate high doses of Cr(VI). Plants were grown semihydroponically with different concentrations of either Cr(III) or Cr(VI). A combination of synchrotron X-ray spectroscopic techniques, scanning electron and light microscopy and infrared spectroscopy were used to determine the distribution and speciation of Cr. *S. vulgaris* accumulated more Cr when grown with Cr(VI) resulting in an overall reduction in biomass. Starch accumulation in leaves may be attributed to an impartment between carbon utilization and assimilation resulted from stunted plant growth but not the complete inhibition of photosynthesis indicating that *S. vulgaris* possess tolerance mechanisms that allows it to survive in Cr(VI) rich environments. These primary tolerance mechanisms are (a) the total reduction of Cr(VI) to Cr(III) in the rhizosphere or just after uptake in the fine lateral root tips and (b) chelation of Cr(III) to the cell wall both of which reduce metal interference with critical cell functions. These mechanisms make *S. vulgaris* suitable for in situ remediation of Cr polluted soils.

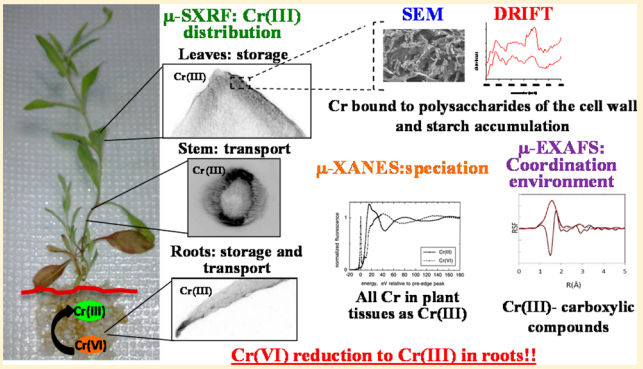

INTRODUCTION

Chromium is a transition metal which represents the seventh most abundant element on earth. Due to its corrosion-resistant properties it is used in many industrial activities. Its world production is in the order of 10 000 000 tons per year.[1] About 90% goes to metallurgical applications, especially into manufacture of stainless steel; 5% is used in chemical manufacturing as leather tanning, pigments and electroplating and the remaining 5% of Cr goes to refractory applications.[1] The wide and increasing use of Cr in industry has led to the disposal and dispersal of large amounts of chromium into soils and waters making it a metal of high environmental concern.

Chromium has several oxidation states ranging from (II) to (VI), the most common and stable forms being Cr(III) and Cr(VI). Cr(VI), an oxyanion (CrO_4^{-2} orCrO_7^{-2}), is repelled by the negative charge of soil, as such, it remains in soil solution or weakly sorbed where it is bioavailable for animals and plants. Because of its solubility, Cr(VI) enters living cells easily where it generates reactive oxygen species (ROS) causing severe oxidative injuries to cell constituents and DNA. In humans it is classified as carcinogen of Group A.[2] Cr(III), however, occurs as a cation which is more readily adsorbed to the negatively charged particles of soils, especially clays and it can also precipitate as insoluble oxide and hydroxide compounds making Cr(III) less soluble and bioavailable than Cr(VI). As such, Cr(III) is between 10 and 100 times less toxic than Cr(VI).[4] Cr(III) may be an essential component responsible for the control of glucose and lipid metabolism in mammals[3] although, this nutritional role is still under question.

In natural soils organic matter acts as an electron donor for Cr(VI) reduction in a process called "dechromification"[5] resulting in Cr(III). However, industrial spills could overwhelm the reductive capacity of soils, especially in alkaline environments where this process is not favored.

Traditional physicochemical cleanup technologies used for the remediation of heavy metal polluted soils are energy intensive, monetarily prohibitive and only applicable for small areas of enriched soils. Further, they generate wastes and hazardous byproducts and destroy soil structure.[6] Phytomanagement of contaminated soils, described as the use of vegetation alone or in combination with other technologies, can be a more cost-effective means of mitigating environmental risks associated with large metal enriched sites.[7] These technologies rely on the ability of plants to tolerate (phytostabilization) and/or accumulate (phytoextraction)

Received: April 29, 2014
Revised: July 24, 2014
Accepted: September 4, 2014
Published: September 4, 2014

   dx.doi.org/10.1021/es502099g | Environ. Sci. Technol. 2014, 48, 11479−11486

large amounts of heavy metals in their tissues. Understanding the mechanisms by which plants take up and detoxify metals is one key factor to increase the efficiency of this technology.

There are only a few studies on the ability of plants to take up and/or reduce Cr(VI) to the less toxic Cr(III) specie.[8−10] Utilization of plant-mediated Cr(VI) reduction could represent an important in situ detoxification method to reduce the risk of Cr(VI) exposure to higher trophic levels. *Silene vulgaris* (Moench) is a perennial dicotyledonous facultative methallophyte with a wide distribution throughout Europe, North America, Asia and North Africa and a proven tolerance to a diversity of metals.[11−13] As a native, noninvasive species *S. vulgaris* is a good candidate for phytomanagement of a variety of polluted sites. Previous studies with clones of *S. vulgaris* have shown the tolerance of this species to Cr[14,15] but more research is necessary to evaluate if this species could be effectively used in Cr contaminated sites. The objectives of this study were (i) to compare Cr uptake and the phenotypic and biochemical changes induced in *S. vulgaris* when grown in Cr(III) or Cr(VI) supplemented media and (ii) to describe the Cr(VI) tolerance pathway for *S. vulgaris*. To achieve these objectives, a combination of X-ray spectroscopic techniques, scanning electron and light microscopy and diffusive reflectance infrared Fourier transform spectroscopy were used.

MATERIALS AND METHODS

Plant Material and Growth Conditions. Seeds of a chromium tolerant population of *S. vulgaris* (Moench) (EC_{100} between 30 and 100 μM Cr(VI), Supporting Information (SI) Figure S1) were germinated and precultured in semi-hydroponics. Plants were then randomly selected for treatment with 30 μM (1.56 mg·L^{-1}) and 60 μM (3.12 mg·L^{-1}) Cr as follows: (a) control, no Cr addition, (b) 30 μM Cr(III), (c) 60 μM Cr(III), (d) 30 μM Cr(VI), and (d) 60 μM Cr(VI). Cr(III) was provided as $Cr(NO_3)_3{\cdot}9H_2O$ and Cr(VI) as $K_2Cr_2O_7$. Doses were selected in order to be environmentally relevant and in the range of tolerance of this specie and at which toxicity-tolerance mechanisms are already activated.[14,15]

Plant Tissue Analysis. After 3 weeks of treatment, roots and shoots were separated and washed thoroughly with water and 0.001 M of $CaCl_2$ to remove weakly sorbed metals, immediately frozen in liquid nitrogen and stored at −80 °C until being freeze-dried. Plant dry weights were recorded prior to being ground and digested in MARS express (CEM, Matthews, North Carolina) microwave digester using method EPA 3052. Digestion sets included duplicate samples, reagent blanks and standard reference plant tissues (SRM 1573a, Tomato leaf, NIST, Gaithursburg, MD). Cr concentrations were determined using an Agilent 7500cxICP-MS (Santa Clara, Ca). Mean recovery of Cr from the SRM was ∼85% of the median acid-leachable value.

Statistical Treatment. Statistical analysis was performed using SPSS version 19.0 (IBM, Armonk, N.Y.). Data from dry weights and Cr concentrations were analyzed using a general lineal model (GLM) with chromium treatment as the experimental factor at α = 0.05 using the F-test. GLM was followed by a post hoc Duncan test to assess the significance of differences among treatments for each variable. The results are shown within the tables as lower case letters in which values not sharing the same letter are significantly different. Values given in the tables indicate mean values (n = 3) ± standard error (S.E.).

Synchrotron-Based X-ray Spectroscopy (μ-SXRF, μ-XANES, and μ-EXAFS). Chromium speciation and element distributions were determined using synchrotron micro X-ray fluorescence spectroscopy (μ-SXRF, μ-XAFS) on beamline 10.3.2 (1.9GeV and 300 mA) at the Advanced Light Source, Lawrence Berkeley National Lab (ALS-LBNL, Berkeley, CA). Fresh plants from the 60 μM Cr(VI) treatment were transported to the beamline where, just prior to analysis, leaves, stems and roots were removed, rapidly frozen in liquid N_2 and mounted on a Peltier cold stage using silica vacuum grease. The stage was maintained −30 °C throughout the experiment. Prior to analysis the beamline was calibrated using a metal foil standard. The sample stage was attached to an x,y,θ stepping stage positioned 45° to the incident X-ray beam. For collecting μ-SXRF maps, the beam energy was set to 11 keV such that the Kα fluorescence line intensities of Cr, Mn, Fe, Zn, Cu, Ni, Ti, As Mg, Ca, and K were detected using a 7-element Canberra Ultra LE-Ge detector (Meriden, CT) positioned 90° to the incident beam. Analysis started by first collecting coarse fluorescence maps using beam sizes from 5 to 16 μm and step sizes between 20 and 5 μm depending on the area mapped and the resolution required. The dwell time was between 20 and 100 ms. The distribution of Cr(VI) and Cr(III) in the plant tissues were initially determined by collecting maps at the energy of maximum absorbance for each Cr species and above the absorption edge of both (5984.00, 5993.00, 6006.00 keV, respectively). After several maps were collected in this fashion it was determined that only Cr(III) was present in the tissues and the subsequent maps were recorded at 11 keV.

Using the μSXRF maps, regions of interest ("hotspots") were identified and μ-XANES and μ-EXAFS spectra were collected at these spots. μ-XANES spectra were collected in fluorescence mode from 50 eV below to 150 eV above Cr k-edge (5989.02 keV) using quick-scanning mode which permitted the collection of a single spectrum in ∼40 s allowing for the detection of any beam induced changes in the Cr oxidation state. One hundred 40 s scans were averaged to make up one spectrum and this procedure repeated approximately 5 times at each hotspot resulting in 5 spectra per hotspot. Prior to averaging each spectrum was background subtracted and normalized before least-squares combination fitting (LCF) using beamline 10.3.2 software. Standard preparation and shell fitting of μ-EXAFS spectra collected from different parts of the plant is described in the SI.

Scanning Electron and Light Microscopy. A Nikon Eclipse 90i light microscope and model S-3200 Hitachi scanning electron microscope equipped with a Princeton Gamma-Tech energy dispersive spectroscopy (EDS) micro-analysis system were used to examine fresh and freeze-fixed samples, respectively, to evaluate the phenotypic changes induced during Cr exposure. For SEM, regular cross sections of lyophilized stem and leaf samples were generated using a surgical blade and the pieces then mounted on-end on an Al stub with carbon adhesive and sputter coated with 2−3 nm of gold prior to analysis. Samples were analyzed using an accelerating voltage of 20 kV at 250−400 magnification and a working distance of 14 mm.

Diffuse Reflectance Infrared Fourier Transform Spectroscopy (DRIFTS). Infrared spectra from the mid-IR region (600−1800 cm^{-1}) were used to evaluate the plant structural or biochemical changes that may have occurred with Cr exposure. A 5% mixture of freeze-dried leaves and roots from each of the treatments were prepared by grinding and thoroughly mixing

with potassium bromide (KBr). Infrared spectra were recorded using a Thermo Scientific Nicolet 6700 FTIR equipped with a Smart collector diffuse reflectance accessory and MCT/A detector. Each sample spectra is an average of 254 spectra collected with 4 cm^{-1} resolution.

RESULTS AND DISCUSSION

Plant Growth and Cr Uptake. Dry mass reduction in shoots from plants grown in 30 μM Cr(III) and Cr(VI) are similar (~20%) (Table 1). There was a significant decrease in shoot biomass (~40%) in plants grown with 60 μM Cr(VI). In roots, though not statistically significant, there was a similar reduction in root biomass (~24%) in plants grown with 30 and 60 μM Cr(III) and the lower dose of Cr(VI), however the 60 μM Cr(VI) treatment resulted in ~40% reduction in root biomass. Overall, Cr(VI) was the most inhibitory to whole plant (root+shoot) dry matter yield, as has been observed in other species.[16]

Table 1. Percentage of Dry Weights with Respect to the Control and Total Chromium Concentration in Dry Tissues in Shoots and Roots of *S. vulgaris* Exposed to 30 and 60μM of Cr(III) and Cr(VI)[a]

	dry weight (% of control)		μg Cr g^{-1}DW	
treatment	shoot	roots	shoot	root
control	100%^{a}	100%^{ns}	0.45 ± 0.21^{c}	0.75 ± 0.32^{d}
30 μM Cr(III)	85 ± 10 %^{a}	70 ± 14 %^{ns}	2.19 ± 0.87^{c}	105.00 ± 18.02^{cd}
60 μM Cr(III)	120 ± 8 %^{a}	78 ± 11 %^{ns}	4.32 ± 0.94^{c}	186.39 ± 49.45^{c}
30 μM Cr(VI)	81 ± 11 %^{b}	79 ± 15 %^{ns}	51.26 ± 7.93^{b}	926.08 ± 109.08^{b}
60 μM Cr(VI)	59 ± 7%^{b}	58 ± 17 %^{ns}	73.50 ± 10.39^{a}	1155.11 ± 76.70^{a}

[a]Different lowercase letters indicates significant differences between chromium treatments. (Duncan's test $p < 0.05$, mean ± SE, $n = 3$).

Total Cr concentrations were significantly greater in the shoots of plants grown with Cr(VI), especially at the higher dose, compared to those of the controls and plants grown in Cr(III) (Table 1). The highest concentrations in the roots were found in plants grown in Cr(VI), with significantly more in the 60 μM Cr(VI) treatment. Chromium mainly accumulated in roots and was poorly translocated to the shoots in all treatments which has been described as a mechanism by plants to prevent Cr toxicity.[17,18] Irrespective of concentration, plants grown with Cr(III) retained 43−48× more Cr in their roots compared to their shoots, while 16−18× more Cr was retained in the roots of the plants grown with Cr(VI). The greater uptake of Cr in *S. vulgaris* grown with Cr(VI) compared to Cr(III) has been ascribed to the active uptake of Cr(VI) in metabolically driven processes using the same transporters used for essential anions such as sulfate.[19] In contrast, the Cr(III) ion can bind strongly to ion exchange sites of the cell wall within the root apoplast and is only passively taken up.[19]

Spatial Distribution and Speciation of Cr in *S. vulgaris*. Oxidation state μ-SXRF mapping revealed only Cr(III) was present in the roots from plants grown with Cr(VI). XAS spectra from plant samples grown with Cr(VI) show a pre-edge feature similar to that of Cr(III) model compounds (SI Figures S3 and S7). In the +6 oxidation state Cr is in 4-fold, tetrahedral coordination (e.g., CrO_4^{2-}) indicated by a diagnostic large pre-edge peak in the XANES spectra due to the 1s to 3d electron transition. When in the +3 oxidation state Cr forms complexes with 6-fold, octahedral coordination, in which case the diagnostic pre-edge peak is notably smaller and is located at slightly lower energy.[8] Best LLSF of the all μ-EXAFS spectra (SI Table S1) from spots in the roots, stem and shoots were achieved using six first shell oxygen atoms at R_{Cr-O} = 1.98 Å confirming that Cr in all tissues is in octahedral coordination.

The presence of only Cr(III) in plants grown with Cr(VI) has been observed in other species[8,10,20] and is thought to represent an important detoxification pathway for plants. The mechanism by which Cr(VI) is reduced to Cr(III) and whether this happens outside or within the plant are still not known. Cr(VI) shares the same membrane bound transporters as sulfate which leads to more Cr entering the root cells when plants are grown with Cr(VI). Once past the plasma membrane, some researchers hypothesize Cr(VI) reduction is mediated by Fe(III)-reductase enzymes[21−23] supported by the fact that Cr supplied to Fe-deficient plants increases the activity of root associated Fe(III)-reductase[24] which increases the availability of Fe to plants.[25] Alternatively, specific chromate reductases have been isolated in bacteria[26] and some researchers postulate that a similar enzyme may be present in plants.[1,26,27] Reduction of Cr(VI) to Cr(III) could also occur within the rhizosphere promoted by the lower pH, higher root-derived organic C concentrations, and greater microbial and root respiration within this region.[28] There is evidence that reduction of Cr(VI) by organic acids commonly found in root exudates (e.g., citrate, malate) can by catalyzed by soil surfaces[29−33] and if it remains in a complex with the organic ligand may be available for uptake directly or via ligand exchange.[10] Previous studies have shown that exposure to Cr(VI) resulted in increased C concentrations in root exudates from *S. vulgaris*[14] which could have resulted in the abiotic reduction of Cr(VI) to Cr(III), chelation of Cr(III) to organic acids in root exudates, and/or growth promotion of reductive bacteria in the rhizosphere, all of which could lead to uptake of Cr(III).

Cr(III) was found throughout the root system particularly in the root tips (Figures 1.f and 1.i) possibly eluding to a greater importance of root tips in the process of reducing and taking up Cr as shown in other species.[9,27,28] Many of the root tips were collapsed and in some cases curled (Figure 1.i and SI Figure S2) as observed in other plants grown with Cr(VI).[34−36] Root tip deformation is attributed to the oxidizing power of Cr(VI) when in direct contact with the roots leading to plasmolysis of root cells and leakage of the cell contents.[37] The meristematic zone of the root is less suberized and more permeable to Cr and is therefore more sensitive to Cr exposure resulting in irregular cell wall profiles and retraction of the plasma membrane.[36,38] Both the direct effect on root structure and chromosomal aberrations induced by Cr in root cells causes the inhibition of cell division[34] and extension of the cell cycle[39] which likely contributes to root growth retardation found in the 60 μM Cr(VI) treated plants and the decrease in shoot dry mass due to the inability of roots to absorb nutrients and water.[40] The μ-XANES data indicate that a greater portion of the Cr in the root tips (spots 5 and 6 Figure 1 and Table 2) to be in the hydrated and weakly ligated forms (e.g., hexaquo and malonate). Best NLLSF of the μ-EXAFS spectra (SI Table S1) from a spot at the root tip (spot S10 SI Figure S4 and Table

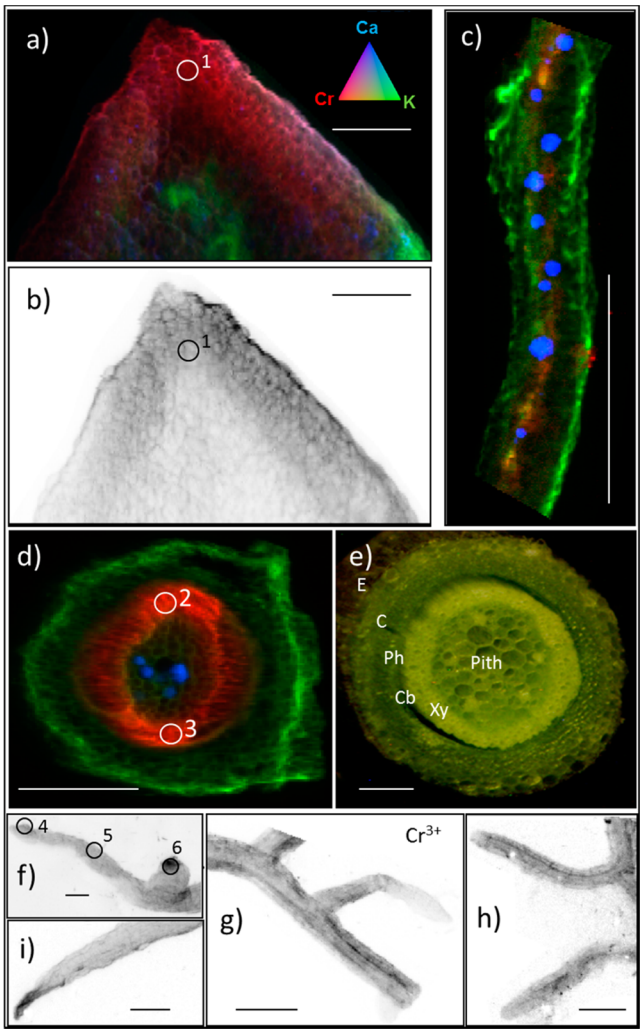

Figure 1. Micro synchrotron X-ray fluoresce (μSXRF) maps showing the distribution of Cr(III) (red), K (green) and Ca (blue) in (a) leaf surface, (c) leaf cross section, and (d) stem cross section from *S. vulgaris* grown 3 weeks in 60 μM Cr(VI). Panels (b) and (f–i) are μ-SXRF maps showing the distribution of Cr(III) only (black) in the same leaf in panel a) and in roots, respectively. Circles correspond to spots where μ-XANES and/or μ-EXAFS spectra were collected. Light microscope image of stem cross-section e) showing the E: epidermis, C: cortex, Ph: phloem, Cb: cambium, Xy: xylem and P: pith. The bar in all panels = 100 μm.

S1) confirmed this finding in that only a first shell O (CN_{Cr-O} = 5.23 at R_{Cr-O} = 1.98 Å) could be fit.

Moving back from the root tip, Cr appears to outline the root cells (SI Figure S2) where it is likely bound to the cell wall, as has been observed in other studies.[10,41] Cr also appears to be in the vascular tissues or concentrated at the endodermis indicated by the pattern of Cr following the trajectory of the root (Figure 1.g and h). Cr uptake occurs across the radius of the root,[42] where at low doses it is preferentially retained in the root cortex. At higher concentrations Cr crosses the endodermis via the symplast and is transported to the upper parts of the plant.[28,43] In these regions away from the root tip (spot 4 Figure 1 and Table 2) the LCF of the μ-XANES data shows that the speciation is dominated by stronger ligands (e.g., acetate or citrate). Supporting the μ-XANES data, NLLSF of the μ-EXAFS spectra (SI Table S1) from a spot just above the root tip (S9 in Figure 4 and SI Figure S4 and Table S1) was achieved using 6 oxygen atoms in the first shell (CN_{Cr-O} = 6 at R_{Cr-O} = 1.98 Å) and approximately 6 carbon atoms in the second shell (CN_{Cr-C} = 5.7 at R_{Cr-C} = 3.36 Å) which resembles that of the Cr(III)-citrate or Cr(III)-malate standards. The data show that Cr has already been reduced to Cr(III), it is concentrated in many of the root tips in a weakly ligated form and away from the root tips it is in strongly ligated forms either for transport in the vascular system or in association with the plant cell wall or exchange sites in the apoplast.

Within the stem, Cr(III) was found in the xylem (Figure 1.d, 1.e and SI Figure S5) but absent from the phloem and the other tissues outside of the vascular elements. LCF of the μ-XANES data from the stems indicate that Cr is primarily in the hydrated and more soluble ligated forms with only one spot showing a small amount of Cr(III) acetate (Table 2). Only a first shell of O (CN_{Cr-O} = 6 at R_{Cr-O} = 1.98 Å) could be confidently fit to all the μ-EXAFS spectra collected from the stem (SI Table S1, Figure S9). These data indicate that the stem is used for Cr transport and not storage in *S. vulgaris*.

Cr(III) was mainly observed in the mesophyll (both palisade and spongy) of the leaf and was absent from the other leaf tissues (Figure 1.c). In the leaf tips (Figure 1.a and b and SI Figure S6), Cr(III) clearly outlines the cells where it appears to be stored in the cell wall or apoplastic space; a pattern that is especially evident in the leaf margins. Margins of the older leaves also appeared red as was observed in Subterranean clover[10] and had lower K and Ca fluorescence intensity (Figure 1.a) indicating that these elements were less concentrated in this region. Chromium did not appear to accumulate in the vascular system of the leaves although they did contain discrete spots of Ca (Figure 1.b) as was also seen in the stem (Figure 1.d and SI Figure S5). The μ-XANES data showed that a greater proportion of Cr in the leaves is in the more strongly ligated forms (Cr(III)-acetate and Cr(III)-citrate) compared to the root and stem tissues (Table 2). It was possible to fit a second shell carbon (CN_{Cr-C} = 4.58 at R_{Cr-C} = 3.34) in one of the three μ-EXAFS scans from a leaf tip (Spot S1, SI Table S1 and Figures S6 and S9), and much like in the root, the fit resembles those for the Cr(III)-citrate or Cr(III)-malate standards.

In plants, organic acids are known to play an important role in metal tolerance, transport through the xylem and vacuolar sequestration[44] and have been found to form stable complexes with Cr(III).[29] Previous studies on Cr speciation in a variety of plant species found Cr(III) bound with oxalate, citrate, malate, and/or acetate ligands.[9,10,27,28,45] Higher concentrations of malate and citrate were found in Zn tolerant genotypes of *S. vulgaris*[46] and, while they were not shown to be directly involved in Zn transport or storage, based on our results, they could potentially play a role in Cr homeostasis. The microfocused techniques used in this study allowed us to interrogate specific regions within *S. vulgaris* and in doing so we found Cr(III) speciation to be different depending on the organ analyzed which was related to whether Cr was being transported or stored.

Based on the LLSF of standards used in this study, Cr(III)-citrate and Cr(III)-malate were indistinguishable from each other, as were the Cr(III)-hexaquo, Cr(III)-malonate, and Cr(III)-tartrate standards. Because of the realized uncertainties associated with coordination number and bond distance estimates from shell fitting of EXAFS data together with the similarity of XANES spectra for many of the Cr species ligated to carboxylic acid groups on organic acids, we were only able to

Table 2. Linear Least Squares Combination Fitting for μXANES Spectra Collected from Leaf, Stem and Root Samples From *S. vulgaris* Grown in 60μM Cr(VI)[a]

	Cr(III)-acetate	Cr(III)-citrate	Cr(III)-malonate	Cr(III)-hexaquo	Cr(III)-oxalate		
sample			%			SUM	NSS
LeafTip1 Spot1 (1)	28.9	37.6	0.0	30.5	0.0	97.0	7.86×10^{-05}
LeafTip2 Spot1 (S2)	28.8	44.4	0.0	19.8	17.5	110.5	4.26×10^{-04}
LeafTip3 Spot1 (S3)	34.4	36.1	0.0	24.0	0.0	95.0	9.41×10^{-05}
leaf avg. =	28.9	41.0	0.0	25.2	8.8	103.8	-----
Stem2 Spot2(S5)	17.5	38.1	0.0	42.7	0.0	98.3	1.75×10^{-04}
Stem3 Spot2 (S7)	0.0	31.3	21.7	40.7	0.0	93.7	3.22×10^{-04}
Stem3 Spot1 (S8)	0.0	38.0	29.3	38.8	0.0	106.1	2.03×10^{-04}
stem avg. =	5.8	35.8	17.0	40.7	0.0	99.3	-----
Root4 Spot4 (4)	36.3	30.1	0.0	37.1	0.0	103.5	1.20×10^{-04}
Root4 Spot3 (5)	26.7	0.0	34.4	41.7	0.0	102.8	1.02×10^{-04}
Root4 Spot1 (6)	0.0	27.1	16.4	54.9	0.0	98.4	1.04×10^{-04}
root avg. =	21	19.0	16.8	45.6	0.0	102.1	
overall avg. =	18.5	24.1	18.7	35.9	2.9	100.1	

[a]Value in parentheses after the sample name corresponds to points in the μ-SXRF maps where the spectra were taken (S = Supporting Information).

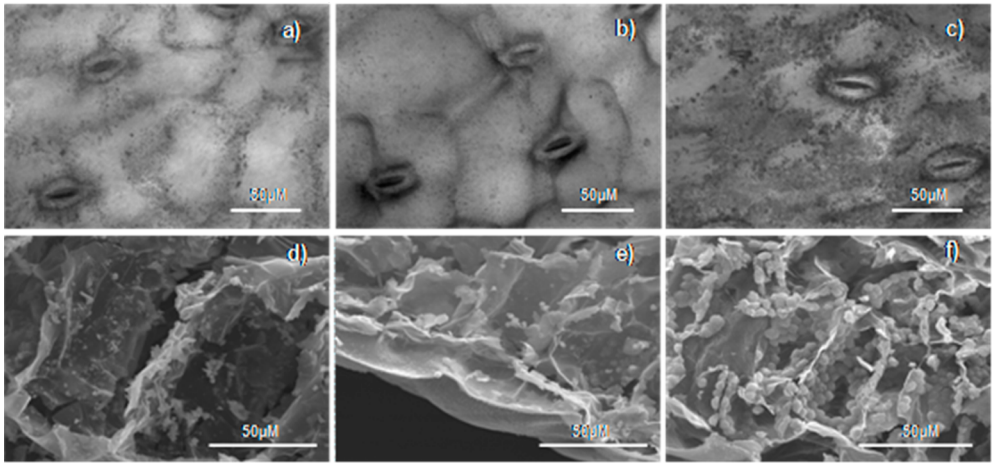

Figure 2. Light microscopy images of *S. vulgaris* fresh leaf surfaces from a) control, (b) 60 μM Cr(III), and (c) 60 μM Cr(VI) treated plants. Scanning electron micrographs of *S. vulgaris* leaf cross sections showing palisade mesophyll cells from (d) control plants, (e) 60 μM Cr(III) treated plants, (f) 60 μM Cr(VI) treated plants.

reliably differentiate between Cr(III)-oxalate, Cr(III)-acetate, Cr(III)-malate/Cr(III)-citrate, and the other Cr(III) standards evaluated. For this reason, and together with our observation of where Cr is located in the plant tissues, we interpreted LCF where Cr(III)-acetate and/or Cr(III)-oxalate were identified and where LLSFs showed a strong second shell C contribution to indicate more strongly ligated Cr as might be found when Cr is bound to the plant cell wall of leaf tips, while fits indicating hexaquo-Cr(III) (and related species) to represent weakly ligated Cr species as might be found in the stem xylem.

Phenotypic Changes and Biochemical Effects of Cr in Leaves of *S. vulgaris*. Dense granular precipitates were observed in light microscope (Figure 2.c) and SEM micrographs (Figure 2.f) of leaves from plants grown with 60 μM Cr(VI), but absent in leaves from control plants and those grown with Cr(III) (Figure 2.a,b and 2.d,e). The region of the IR spectrum between 1200 and 1000 cm^{-1}, is considered diagnostic for cell wall polysaccharides (e.g., pectin, cellulose, hemicellulose). This region includes the absorption bands associated with C−O stretching of starch (1150−980 cm^{-1}),[47] which increased dramatically in intensity in leaves of plants from the 60 μM Cr(VI) treatment but change little for plants grown with either concentration of Cr(III) or the lower concentration of Cr(VI). At high Cr(VI) concentrations more Cr gets into the plant and is transported to the leaves compared to the other treatments and in response we observed reduced plant biomass and what appears to be an increase in starch accumulation in *S. vulgaris*. Accumulation of starch in leaves due to Cr(VI) treatments has been related to the duration and concentration of Cr(VI) exposure.[48−50] Rodriguez et al. (2012) found that biochemical processes were affected by lower concentrations of Cr(VI) while photochemical efficiency was compromised at higher dosages in *Pea sativum*.[50] Thus, starch accumulation in leaves of *S. vulgaris* may be attributed to an impartment between carbon utilization and assimilation that takes places at higher Cr(VI) doses at which plant growth is stunted but photosynthesis is not yet completely inhibited.

There were significant changes in the 1200−1500 cm^{-1} region of the FTIR spectra for both Cr(VI) treatments which are diagnostic for cell wall components and may be indicative of the mechanism of Cr tolerance in *S. vulgaris* leaves. Proteins, amino acids and phenolics play a role in sequestration of metals in the cell wall, however it is the amount of polysaccharides rich in carboxyl groups that are thought to be most important at

dictating the capacity of the cell wall to bind divalent and trivalent cations.[51] Though overlap of bands in this region makes it difficult to assign bands to specific cell wall components, spectra from leaves of control plants had bands at 1319 cm^{-1} and at 1383 cm^{-1} which may be attributed to xyloglucan (Figure 3); the most abundant hemicellulose in the

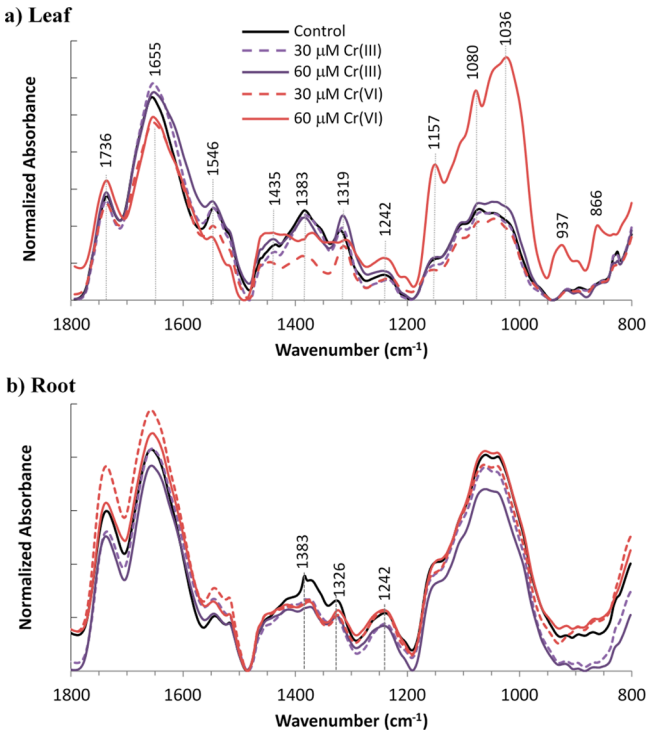

Figure 3. Diffuse reflectance infrared Fourier transform (DRIFT) spectra of a) leaves and b) roots of *S. vulgaris* treated 3 weeks with different concentrations and forms of chromium. Peak labels are based on the control spectra.

primary cell wall of dicots and nongraminaceous monocots.[52] The intensity of these bands diminished in the 30 μM Cr(VI) treatment or vanished and shifted to lower wavenumbers in the 60 μM Cr(VI) treatment. The suppression of these bands indicates alteration of CH_2 groups of this cell wall structural component likely caused by greater concentrations of Cr(III) in the leaves of Cr(VI) treated plants.

In roots, the IR spectra are similar in all Cr treatments irrespective of Cr concentration or species. Slight suppression of bands between 1200 and 1500 cm^{-1} is observed with respect to the control, specifically the band at 1383 cm^{-1} (Figure 3). Cell wall binding has been described as the primary mechanism used by *S. vulgaris* to tolerate increased metals.[53] Our findings from IR together with the XAS data from roots, suggest the first mechanism used to protect against Cr toxicity is retention of Cr in the roots, a portion of which is bond to the cell wall in the apoplastic space of the root cortex. Then, at higher rhizosphere concentrations more Cr is transported to the leaves where it appears to bind to the cell wall in the symplastic space. Because the cell wall composition differs in the roots compared to the shoots (evident when comparing the IR spectra of the leaves and roots of the controls), how the Cr binds may therefore be different as well.

Further evidence for Cr binding to the cell wall may come from the buildup of Ca in the leaf and stem vasculature. There were discrete angular spots of Ca in the phloem tissues of the stem and leaf veins (blue in Figure 1.c and d). Increasing amounts of Ca in *S. vulgaris* plants exposed to Cr(VI) has been observed in our lab (unpublished) and in *Oryza sativa* and *Salsola kali*.[54,55] Some researchers have found Ca in association with heavy metals in plant tissues and attributed the formation of Ca-heavy metal grains as a way of preventing the metal from entering the cytoplasm.[56,57] However, in this study we saw no colocalization of Cr with Ca in our SXRF maps (Figure 1) or EDAX spectra (data not shown) collected from these spots. Several studies examining the biosorption of heavy metals onto cell wall pectins found that metal exposure resulted in release of Ca from the pectin in what is interpreted as ion exchange between the bridging Ca and metal ion.[58−60] Retention of Cr(III) on the cation exchange sites of the vessel walls by a transport mechanism similar to that of Ca^{2+} has been previously described.[37] Thus, Ca accumulations found in the μ-SXRF maps could be due to the displacement of Ca by Cr^{3+} in the cell wall. As such, the association of Cr with the cell wall in the SXRF micrographs, the XAS fits indicating stronger complexes with carboxylic compounds in these areas, FTIR spectra indicating alteration of cell wall polysaccharides, and the buildup of Ca in the vasculature provides some of the strongest evidence that Cr in *S. vulgaris* is bound to the cell wall. The stiffening of the cell wall as a result of metal binding could inhibit cell elongation[61,62] which, together with the process mentioned previously, could explain the growth retardation observed in the Cr treated plants.

In summary, the difference in oxidizing power and uptake of Cr(VI) vs Cr(III) resulted in more Cr accumulation and growth retardation in *S. vulgaris* exposed to Cr(VI). However, starch accumulation in the plants grown with Cr(VI) indicates that *S. vulgaris* is still able to fix C suggesting that it possess tolerance mechanisms enabling it to survive when grown with Cr(VI). The main process implicated in tolerance is the total reduction of Cr(VI) to less toxic Cr(III) within the rhizosphere or immediately after uptake by the roots where it is bound to the root cell wall in the apoplastic space. Then, Cr is transported in the stem by more weakly ligated forms and sequestered in the cell wall of leaf margins where it does not interference with photosynthetically active tissues. To date, the study of Cr chelation, transport and storage in plants has largely relied on homogenized samples and highlight the role of organic acids in Cr uptake and storage. To our knowledge, this is the first study to use micro X-ray fluorescence spectroscopy to study the speciation and localization of Cr in fresh-hydrated tissues. Results from this study provides new insight into the important role the cell wall plays in Cr chelation and tolerance. This work shows that, from the point of view of environmental cleanup, revegetation with *S. vulgaris* provides a green alternative for in situ detoxification of Cr(VI) to stable and less toxic Cr(III) making *S. vulgaris* a viable species for use in the phytostabilization of Cr polluted soils.

■ ASSOCIATED CONTENT

Supporting Information

Supporting Information provides the description of tolerance test (S1), plant culture (S2) and of linear least-squares fitting procedure (S3). Additional μ-SXRF micrographs of roots (S7, S9), stem (S10), and leaf tips (S11), and results from Linear Least Squares Fit of μ-XANES (S8, S12) and μ-EXAFS (S13−15) spectra of standards and samples are also provided in this section.This material is available free of charge via the Internet at http://pubs.acs.org.

AUTHOR INFORMATION

Corresponding Author

*E-mail: ana.pradas@ujf-grenoble.fr.

Present Address

§Geochemistry 4D group, ISTerre, Université Joseph Fourier, BP 53, 38041 Grenoble Cedex 9, France.

Notes

The authors declare no competing financial interest.

ACKNOWLEDGMENTS

The authors thank the financial supports provided by INIA ("Contratación de Doctores" 2007 INIA-CCAA) and IMIDRA for the fellowship of Ana E. Pradas. The authors would also like to thank Jason Unrine for ICP-MS analysis and Joeseph V. Kupper for assistance with lab experiments. The Advanced Light Source is supported by the Director, Office of Science, Office of Basic Energy Sciences, of the U.S. Department of Energy under Contract No. DE-AC02-05CH11231.

REFERENCES

(1) Cervantes, C.; Campos-Garcia, J.; Devars, S.; Gutierrez-Corona, F.; Loza-Tavera, H.; Torres-Guzman, J. C.; Moreno-Sanchez, R. Interactions of chromium with microorganisms and plants. *Fems Microbiol. Rev.* **2001**, *25* (3), 335−347.

(2) USEPA. *Toxicological Review of Hexavalent Chromium*; U.S. Goverment Printing Office: Washington, DC, 1998.

(3) Levina, A.; Lay, P. A. Chemical properties and toxicity of chromium(III) nutritional supplements. *Chem. Res. Toxicol.* **2008**, *21* (3), 563−571.

(4) Deflora, S.; Bagnasco, M.; Serra, D.; Zanacchi, P. Genotoxicity of chromium compounds: A Review. *Mutat. Res.* **1990**, *238* (2), 99−172.

(5) Bartlett, R. J. Chromium cycling in soils and water—Links, gaps, and methods. *Environ. Health Perspect.* **1991**, *92*, 17−24.

(6) Caliman, F. A.; Robu, B. M.; Smaranda, C.; Pavel, V. L.; Gavrilescu, M. Soil and groundwater cleanup: Benefits and limits of emerging technologies. *Clean Technol. Environ. Policy* **2011**, *13* (2), 241−268.

(7) Robinson, B. H.; Banuelos, G.; Conesa, H. M.; Evangelou, M. W. H.; Schulin, R. The phytomanagement of trace elements in soil. *Crit. Rev. Plant Sci.* **2009**, *28* (4), 240−266.

(8) Zayed, A.; Lytle, C. M.; Qian, J. H.; Terry, N. Chromium accumulation, translocation and chemical speciation in vegetable crops. *Planta.* **1998**, *206* (2), 293−299.

(9) Aldrich, M. V.; Gardea-Torresdey, J. L.; Peralta-Videa, J. R.; Parsons, J. G. Uptake and reduction of Cr(VI) to Cr(III) by mesquite (*Prosopis spp.*): Chromate-plant interaction in hydroponics and solid media studied using XAS. *Environ. Sci. Technol.* **2003**, *37* (9), 1859−1864.

(10) Howe, J. A.; Loeppert, R. H.; Derose, V. J.; Hunter, D. B.; Bertsch, P. M. Localization and speciation of chromium in subterranean clover using XRF, XANES, and EPR spectroscopy. *Environ. Sci. Technol.* **2003**, *37* (18), 4091−4097.

(11) Ernst, W. H. O.; Nelissen, H. J. M.; Bookum, W. M. T. Combination toxicology of metal-enriched soils: Physiological responses of a Zn and Cd resistant ecotype of *Silene vulgaris* on polymetallic soils. *Environ. Exp. Bot.* **2000**, *43*, 55−71.

(12) Jack, E. M.; Anatasova, S.; Verkleij, J. A. C. Callus induction and plant regeneration in the metallophyte *Silene vulgaris* (Caryophyllaceae). *Plant Cell Tissue Organ Cult.* **2005**, *80* (1), 25−31.

(13) Paliouris, G.; Hutchinson, T. C. Arsenic, cobalt and nickel tolerances in two populations of *Silene vulgaris* (Moench) Garcke from Ontario, Canada. *New Phytol.* **1991**, *117* (3), 449−459.

(14) Pradas del Real, A. E.; García-Gonzalo, P.; Lobo, M. C.; Pérez-Sanz, A. Chromium speciation modifies root exudation in two genotypes of *Silene vulgaris*. *Environ. Exp. Bot.* **2014**, *107*, 1−6.

(15) Pradas-del-Real, A. E.; Garcia-Gonzalo, P.; Alarcon, R.; Gonzalez-Rodriguez, A.; Lobo, M. C.; Perez-Sanz, A. Effect of genotype, Cr(III) and Cr(VI) on plant growth and micronutrient status in *Silene vulgaris* (Moench). *Span. J. Agric. Res.* **2013**, *11* (3), 685−694.

(16) Shanker, A. K.; Djanaguiraman, M.; Venkateswarlu, B. Chromium interactions in plants: Current status and future strategies. *Metallomics.* **2009**, *1* (5), 375−383.

(17) McGrath, S. P. The uptake and translocation of tri-valent and hexa-valent chromium and effects on the growth of oat in flowing nutrient solution and in soil. *New Phytol.* **1982**, *92* (3), 381−390.

(18) Sharma, D. C.; Sharma, C.; Tripathi, R. D. Phytotoxic lesions of chromium in maize. *Chemosphere.* **2003**, *51* (1), 63−68.

(19) Skeffington, R. A.; Shewry, P. R.; Peterson, P. J. Chromium uptake and transport in barley seedlings (*Hordeum vulgare* L). *Planta.* **1976**, *132* (3), 209−214.

(20) Zhao, Y.; Parsons, J. G.; Peralta-Videa, J. R.; Lopez-Moreno, M. L.; Gardea-Torresdey, J. L. Use of synchrotron and plasma-based spectroscopic techniques to determine the uptake and biotransformation of chromium(III) and chromium(VI) by *Parkinsonia aculeata*. *Metallomics* **2009**, *1* (4), 330−338.

(21) Zayed, A.; Terry, N. Chromium in the environment: Factors affecting biological remediation. *Plant Soil* **2003**, *249* (1), 139−156.

(22) Santana, K. B.; de Almeida, A.-A. F.; Souza, V. L.; Mangabeira, P. A. O.; Silva, D. d. C.; Gomes, F. P.; Dutruch, L.; Loguercio, L. L. Physiological analyses of *Genipa americana* L. reveals a tree with ability as phytostabilizer and rhizofilterer of chromium ions for phytoremediation of polluted watersheds. *Environ. Exp. Bot.* **2012**, *80*, 35−42.

(23) Singh, H. P. Chromium toxicity and tolerance in plants. *Environ. Chem. Lett.* **2013**, *11* (3), 229−254.

(24) Schmidt, W. Influence of chromium(lll) on root-associated Fe(lll) reductase in *Plantago lanceolata* L. *J. Exp. Bot.* **1996**, *47* (6), 805−810.

(25) Bonet, A.; Poschenrieder, C.; Barcelo, J. Chromium III-iron interaction in Fe-deficient and Fe-sufficient bean plants. I. Growth and nutrient content. *J. Plant Nutr.* **1991**, *14* (4), 403−414.

(26) Opperman, D. J.; van Heerden, E. A membrane-associated protein with Cr(VI)-reducing activity from *Thermus scotoductus* SA-01. *FEMS Microbiol. Lett.* **2008**, *280* (2), 210−218.

(27) Lytle, C. M.; Lytle, F. W.; Yang, N.; Qian, J. H.; Hansen, D.; Zayed, A.; Terry, N. Reduction of Cr(VI) to Cr(III) by wetland plants: Potential for in situ heavy metal detoxification. *Environ. Sci. Technol.* **1998**, *32* (20), 3087−3093.

(28) Bluskov, S.; Arocena, J. M.; Omotoso, O. O.; Young, J. P. Uptake, distribution, and speciation of chromium in *Brassica juncea*. *Int. J. Phytoremediat.* **2005**, *7* (2), 153−165.

(29) Srivastava, S.; Prakash, S.; Srivastava, M. M. Chromium mobilization and plant availability—The impact of organic complexing ligands. *Plant Soil.* **1999**, *212* (2), 203−208.

(30) Sarkar, B.; Naidu, R.; Krishnamurti, G. S. R.; Megharaj, M. Manganese(II)-catalyzed and clay-minerals-mediated reduction of chromium(VI) by citrate. *Environ. Sci. Technol.* **2013**, *47* (23), 13629−13636.

(31) Zhong, L. Y.; Yang, J. W. Reduction of Cr(VI) by malic acid in aqueous Fe-rich soil suspensions. *Chemosphere* **2012**, *86* (10), 973−978.

(32) Yang, J. W.; Zhong, L. Y.; Liu, L. M. Coupling of tartaric acid-promoted soil dissolution and Cr(VI) reduction in an oxisol. *J. Geochem. Explor.* **2013**, *125*, 138−143.

(33) Yang, J. W.; Guo, R. F.; Chen, S. Q.; Li, L. T. Interaction between Cr(VI) and a Fe-rich soil in the presence of oxalic and tartaric acids. *Environ. Geol.* **2008**, *53* (7), 1529−1533.

(34) Liu, D. H.; Jiang, W. S.; Li, M. X. Effects of trivalent and hexavalent chromium on root growth and cell division of *Allium cepa*. *Hereditas* **1992**, *117* (1), 23−29.

(35) Zou, J. H.; Wang, M.; Jiang, W. S.; Liu, D. H. Effects of hexavalent chromium (VI) on root growth and cell division in root tip cells of *Amaranthus viridis* L. *Pak. J. Bot.* **2006**, *38* (3), 673−681.

(36) di Toppi, L. S.; Fossati, F.; Musetti, R.; Mikerezi, I.; Favali, M. A. Effects of hexavalent chromium on maize, tomato, and cauliflower plants. *J. Plant Nutr.* **2002**, *25* (4), 701−717.
(37) Vazquez, D.; Poschenrieder, C.; Barcelo, J. Chromium-VI induced structural and ultrastructural changes in bush bean-plants (*Phaseolus vulgaris* L). *Ann. Bot.* **1987**, *59* (4), 427−438.
(38) Samantary, S. Biochemical responses of Cr-tolerant and Cr-sensitive mung bean cultivars grown on varying levels of chromium. *Chemosphere* **2002**, *47* (10), 1065−1072.
(39) Sundaramoorthy, P.; Chidambaram, A.; Ganesh, K. S.; Unnikannan, P.; Baskaran, L. Chromium stress in paddy: (i) Nutrient status of paddy under chromium stress; (ii) Phytoremediation of chromium by aquatic and terrestrial weeds. *C. R. Biol.* **2010**, *333* (8), 597−607.
(40) Hayat, S.; Khalique, G.; Irfan, M.; Wani, A. S.; Tripathi, B. N.; Ahmad, A. Physiological changes induced by chromium stress in plants: An overview. *Protoplasma.* **2012**, *249* (3), 599−611.
(41) Mangabeira, P. A.; Ferreira, A. S.; de Almeida, A.-A. F.; Fernandes, V. F.; Lucena, E.; Souza, V. L.; dos Santos Junior, A. J.; Oliveira, A. H.; Grenier-Loustalot, M. F.; Barbier, F.; Silva, D. C. Compartmentalization and ultrastructural alterations induced by chromium in aquatic macrophytes. *Biometals.* **2011**, *24* (6), 1017−1026.
(42) Mangabeira, P. A.; Gavrilov, K. L.; de Almeida, A. A. F.; Oliveira, A. H.; Severo, M. I.; Rosa, T. S.; Silva, D. D.; Labejof, L.; Escaig, F.; Levi-Setti, R.; Mielke, M. S.; Loustalot, F. G.; Galle, P. Chromium localization in plant tissues of *Lycopersicum esculentum* Mill using ICP-MS and ion microscopy (SIMS). *Appl. Surf. Sci.* **2006**, *252* (10), 3488−3501.
(43) Shanker, A. K.; Cervantes, C.; Loza-Tavera, H.; Avudainayagam, S. Chromium toxicity in plants. *Environ. Int.* **2005**, *31* (5), 739−753.
(44) Clemens, S. Molecular mechanisms of plant metal tolerance and homeostasis. *Planta* **2001**, *212* (4), 475−486.
(45) Montes-Holguin, M. O.; Peralta-Videa, J. R.; Meitzner, G.; Martinez-Martinez, A.; De la Rosa, G.; Castillo-Michel, H. A.; Gardea-Torresdey, J. L. Biochemical and spectroscopic studies of the response of *Convolvulus arvensis* L. to chromium(III) and chromium(VI) stress. *Environ. Toxicol. Chem.* **2006**, *25* (1), 220−226.
(46) Harmens, H.; Koevoets, P. L. M.; Verkleij, J. A. C.; Ernst, W. H. O. The Role of Low Molecular Weight Organic Acids in the Mechanism of Increased Zinc Tolerance in *Silene Vulgaris* (Moench) Garcke. *New Phytol.* **1994**, *126* (4), 615−621.
(47) Stewart, D. Fourier transform infrared microspectroscopy of plant tissues. *Appl. Spectrosc.* **1996**, *50* (3), 357−365.
(48) Rai, V.; Mehrotra, S. Chromium-induced changes in ultra-morphology and secondary metabolites of *Phyllanthus amarus* Schum & Thonn—An hepatoprotective plant. *Environ. Monit. Assess.* **2008**, *147* (1−3), 307−315.
(49) Nichols, P. B.; Couch, J. D.; Al-Hamdani, S. H. Selected physiological responses of *Salvinia minima* to different chromium concentrations. *Aquat. Bot.* **2000**, *68* (4), 313−319.
(50) Rodriguez, E.; Santos, C.; Azevedo, R.; Moutinho-Pereira, J.; Correia, C.; Dias, M. C. Chromium (VI) induces toxicity at different photosynthetic levels in pea. *P Plant Physiol. Biochem.* **2012**, *53*, 94−100.
(51) Krzeslowska, M. The cell wall in plant cell response to trace metals: Polysaccharide remodeling and its role in defense strategy. *Acta Physiol. Plant.* **2011**, *33* (1), 35−51.
(52) Alonso-Simón, A.; García-Angulo, P.; Mélida, H.; Encina, A.; Álvarez, J. M.; Acebes, J. L. The use of FTIR spectroscopy to monitor modifications in plant cell wall architecture caused by cellulose biosynthesis inhibitors. *Plant Signal Behav.* **2011**, *6* (8), 1104.
(53) Bringezu, K.; Lichtenberger, O.; Leopold, I.; Neumann, D. Heavy metal tolerance of *Silene vulgaris*. *J. Plant Physiol.* **1999**, *154* (4), 536−546.
(54) Zeng, F.; Ali, S.; Qiu, B.; Wu, F.; Zhang, G. Effects of chromium stress on the subcellular distribution and chemical form of Ca, Mg, Fe, and Zn in two rice genotypes RID C-3348−2011. *J. Plant Nutr. Soil Sci.* **2010**, *173* (1), 135−148.
(55) Gardea-Torresdey, J. L.; de la Rosa, G.; Peralta-Videa, J. R.; Montes, M.; Cruz-Jimenez, G.; Cano-Aguilera, I. Differential uptake and transport of trivalent and flexavalent chromium by tumbleweed (*Salsola kali*). *Arch. Environ. Contam. Toxicol.* **2005**, *48* (2), 225−232.
(56) Sarret, G.; Harada, E.; Choi, Y.-E.; Isaure, M.-P.; Geoffroy, N.; Fakra, S.; Marcus, M. A.; Birschwilks, M.; Clemens, S.; Manceau, A. Trichomes of tobacco excrete zinc as zinc-substituted calcium carbonate and other zinc-containing compounds. *Plant Physiol.* **2006**, *141* (3), 1021−1034.
(57) Choi, Y. E.; Harada, E. Roles of calcium and cadmium on Cd-containing intra- and extracellular formation of Ca crystals in tobacco. *J. Plant Biol.* **2005**, *48* (1), 113−119.
(58) Grant, G. T.; Morris, E. R.; Rees, D. A.; Smith, P. J.; Thom, D. Biological interactions between polysaccharides and divalent cations: The egg-box model. *FEBS lett.* **1973**, *32* (1), 195−198.
(59) Carpita, N. C.; Gibeaut, D. M. Structural models of primary cell walls in flowering plants: Consistency of molecular structure with the physical properties of the walls during growth. *Plant J.* **1993**, *3* (1), 1−30.
(60) Caffall, K. H.; Mohnen, D. The structure, function, and biosynthesis of plant cell wall pectic polysaccharides. *Carbohydr. Res.* **2009**, *344* (14), 1879−1900.
(61) Hall, J. L. Cellular mechanism for heavy metal detoxification and tolerance. *J. Exp. Bot.* **2002**, *53* (366), 1−11.
(62) Poschenrieder, C.; Gunse, B.; Corrales, I.; Barcelo, J. A glance into aluminum toxicity and resistance in plants. *Sci. Total Environ.* **2008**, *400* (1−3), 356−368.